Reconfigurable Robotic Platforms for Structural Health Monitoring

S. G. PIERCE, G. PUNZO, G. DOBIE, R. SUMMAN,
C. N. MACLEOD, C. MCINNES, J. BIGGS,
M. MACDONALD and D. BENNET

ABSTRACT

There are numerous examples for remote inspection on industrial plant and civil structures where a rapid preliminary inspection with either a wheeled remote sensing agent (RSA) or a small unmanned aerial vehicle (UAV) removes the need to physically send a person into a potentially dangerous environment (expensive and hazardous), and removes the need for expensive supporting hardware (scaffolding, safety equipment etc). Many such examples are to be found in nuclear, oil and gas and civil structures where a fundamental requirement for monitoring exists.

Since 2003, The University of Strathclyde has been involved with research as part of the *UK Research Centre for Non Destructive Evaluation* (RCNDE) to develop robotic deployment of NDE measurement probes. The use of multiple inspection vehicles (coupled with different sensing modalities), allows for a flexible, reconfigurable, and adaptive approach to remote health monitoring. However to be effective in real inspection applications, effective co-ordination between multiple agents must be integrated into the system, along with accurate positioning. In this paper we discuss using artificial potential fields for formation structuring for NDE robots. A theoretical framework is developed and supported by experimental measurements of simple formation structuring in the laboratory environment using five independent NDE robots.

S.G. Pierce, *Centre for Ultrasonic Engineering (CUE),* Department of Electronic & Electrical Engineering, University of Strathclyde, Royal College Building, 204 George Street, Glasgow G1 1XW.

INTRODUCTION

Ongoing research at University of Strathclyde as part of the UK Research Centre for Non-Destructive Evaluation (RCNDE) [1] has developed a number of robotic delivery platforms (remote sensing agents, RSAs) geared for NDE applications[2] . Initial work[3] focused on the integration of NDE payloads with autonomous wireless robotic agents, and in particular the delivery of multiple payloads employing data fusion techniques[4] for simple inspection tasks. A major challenge that was identified from this research was for the stringent positioning associated with typical NDE requirements. We have reported on this previously[5] where we have employed a variety of positioning methodologies including odometry, inertial, and acoustic GPS, to obtain the best estimate position using a number of different probabilistic filtering approaches[6]. Our current approach continues to employ these techniques, but also adds vision, SLAM approaches[7], photogrammetric and laser tracker measurements to verify the performance of the probabilistic filtering.

Having established sufficiently precise control and location of single robotic agents, our work has recently moved towards investigating the use of multiple agents. The investigation of swarms of interacting robotic agents has rapidly developed to become a major international research activity, driven by the prospect of solving practical problems in new, highly efficient and robust ways. While the end goal of such research is clear, there remain challenges to be overcome before swarming systems can be deployed for real, mission-critical applications such as NDE. Winfield[8] has articulated the key issues concerning the fielding of swarms of robotic agents and coined the term '*swarm engineering*' to capture the requirements of real, as opposed to laboratory or simulation-based swarming. He notes that intended behaviours must be directly provable, along with assurance that unwanted behaviours cannot occur. Such verification issues are common in spacecraft flight formation[9], and the current work reports on our collaboration with our co-authors in the Advanced Space Concepts Laboratory at University of Strathclyde, to develop swarm behavior based on artificial potential functions.

RSA ROBOT HARDWARE -

The current RSA (remote sensing agent) wheeled robotic inspection platform is shown in figure 1. It is a ruggedised two-wheeled differential drive vehicle with a rear jockey wheel. The wheels are constructed from magnetic material thus allowing traction on ferromagnetic surfaces such as carbon steel. Powered by two independent DC motors, the robot has a top speed of 10 cm/s over level surfaces and weighs just under 2kg. Power for the robots is supplied via an onboard Li:Polymer battery giving approximately three hours run time. An embedded microcontroller is used for control, and Wi-Fi communication providing a range of up to 100m. A range of integrated NDE payloads have been developed previously[2] and figure 1 shows a pair of pitch catch air coupled ultrasonic transducers on the left hand robot, and an integrated camera and magnetic flux leakage (MFL) sensor on the right hand robot.

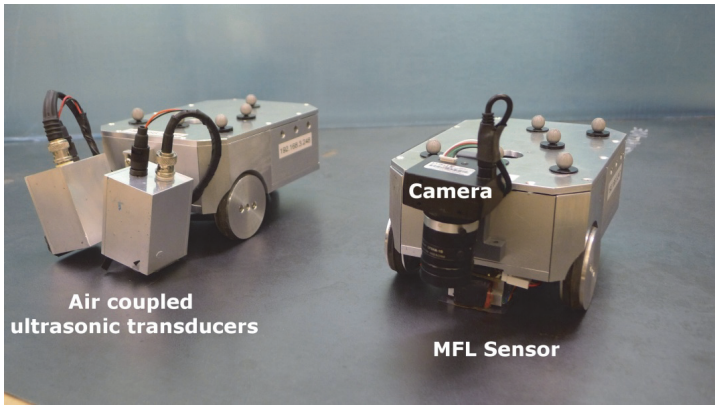

Figure 1. Current generation RSA inspection robots showing pitch-catch air-coupled ultrasonic payload (left) and camera and MFL sensor (right).

A total of five such RSAs were available to investigate the swarming positioning discussed in this paper. The small spherical reflectors visible on the tops of the robots in figure 1 were the reflective markers used by a Vicon T160 motion capture system to track the real time 6 DOF position of each RSA.

SWARM METHODOLOGY

A typical example of a mission-critical application of swarming systems at present is for UAVs operating in a cluttered environment where the system must be validated as safety-critical[10]. Real swarms are engineered artefacts which must reliably perform useful tasks. While biologically inspired, rule-based approaches to swarming, beginning with Reynold's Boids[11] can produce plausible and interesting qualitative behaviours, they will not be acceptable as the kernel for real swarms of robotic agents. The use of physics inspired swarming[12] has been seen as a way of moving towards a more quantitative means of constructing and verifying swarm behavior. For NDE applications the key swarming terminology attributes to consider are *foraging and coverage* and *flocking and formation* [13]. In NDE, foraging and coverage relates to the ability of an agent or set of agents to adequately provide inspection coverage over a given area. Flocking and formation is valuable when considering agent to agent inspection tasks for example pitch catch ultrasonic inspection. For complex agent formations it is even possible to consider complex multi agent ultrasonic and transmission scenarios that implement conventional ultrasonic imaging such as SAFT (synthetic aperture focusing) and FMC and TFM (full matrix capture and total focusing) [14].

In this current paper we concentrate on the methods of artificial potential functions (APF) to implement swarming behavior and will illustrate with simple examples of formation behavior.

Artifical Potential Functions

The RSA velocity field is defined by artificial potential functions based on pair-wise interactions; the Morse potential is used to this end. Two exponential functions provide attractive U_{ij}^{a} and repulsive U_{ij}^{r} components, which are defined as,

$$U_{ij}^{a} = -Ca_{ij} \exp\left[\frac{|x_{ij}|}{La_{ij}}\right] \quad (1)$$

$$U_{ij}^{r} = -Cr_{ij} \exp\left[\frac{|x_{ij}|}{Lr_{ij}}\right] \quad (2)$$

where, Ca_{ij} , Cr_{ij} , La_{ij} and Lr_{ij} are constants and are chosen considering the size of the formation to in which the robots arrange. Subsripts *i j* refer to the contribution to the velocity field of agent *i* due to the proximity of agent *j*; it follows that x_{ij} is defined as $x_i - x_j$, that is, the relative position vector of robot *i* respect to robot *j*.

$$\dot{x}_i^d = -\nabla U_i^a - \nabla U_i^r \quad (3)$$

$$U_i^a = \sum_j U_{ij}^a \qquad U_i^r = \sum_j U_{ij}^r \quad (4)$$

The guidance law provided by the APF just requires the knowledge of relative positions between pairs of agents. The velocity field can then be modified by adding appropriate translational and rotational terms. Here the addition of a rotational one, $\boldsymbol{H_i}$ is considered. It is defined as:

$$\boldsymbol{H_i} = H(\boldsymbol{x_i}) = k_r \boldsymbol{K}(\boldsymbol{x_i} - X) \quad (5)$$

Where X is the position of the centre of mass of the formation; and **K** is the rotation matrix:

$$\boldsymbol{K} = \begin{bmatrix} 0 & -1 \\ 1 & 0 \end{bmatrix} \quad (6)$$

Which rotates the position vector x_i of each agent with respect to the centre of mass of the formation at an angle $\pi/2$. (Here k_r is a constant considered unity).

Hence equation (3) is modified to:

$$\dot{x}_i^d = -\nabla U_i^a - \nabla U_i^r + H_i \quad (7)$$

Symmetric Emergent Behavior

Consider a group of 5 robotic agents controlled through artificial potential function. The emergent clustering structure can take two possible configurations (for simplicity the analysis in this section is referred to Equation 3, without considering any additional terms). The equilibrium condition, characterised by the gradient of $U_i = 0$ for $i = 1, 2.., 5$, is satisfied by two possible arrangements of the robots; a pentagon or a cross. These formations can emerge for Ca_{ij} , Cr_{ij} , La_{ij} , and Lr_{ij} independent from the pair of agents they refer to.

The uncertainty can easily be resolved for the cross scheme; this can be forced by triggering one single parameter Lr_{ij} along the directed edges connecting one agent to the other 4. The 5-agent arrangement can be analysed in terms of the artificial potential gradient sensed by any of them, for instance agent number 1, as shown in Figure 2.

The first derivative of the artificial potential sensed by agent 1 can be calculated for the regular pentagon formation pictured. Then the conditions that apply to the APF coefficients in order to reach a stable equilibrium are deduced. Planar components of the gradient are calculated in Equations (8) and (9).

$$\frac{\partial U_i}{\partial x_i} = \sum_{j=1}^{n} \left[\frac{Ca_{ij}}{La_{ij}} exp\left(- \frac{|x_i - x_j|}{La_{ij}} \right) - \frac{Cr_{ij}}{Lr_{ij}} exp\left(- \frac{|x_i - x_j|}{Lr_{ij}} \right) \right] \frac{x_i - x_j}{|x_i - x_j|} \tag{8}$$

$$\frac{\partial U_i}{\partial y_i} = \sum_{j=1}^{n} \left[\frac{Ca_{ij}}{La_{ij}} exp\left(\frac{|x_i - x_j|}{La_{ij}} \right) \frac{Cr_{ij}}{Lr_{ij}} exp\left(\frac{|x_i - x_j|}{Lr_{ij}} \right) \right] \frac{y_i - y_j}{|x_i - x_j|} \tag{9}$$

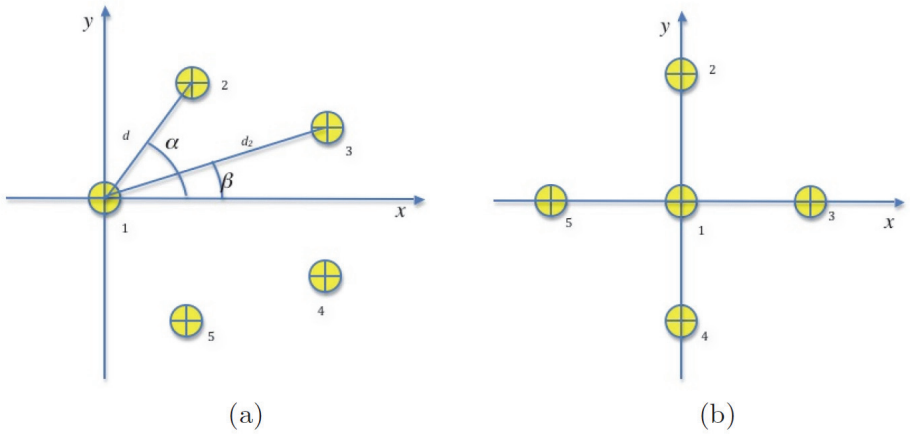

Figure 2. A formation of 5 agents arranged in (a) pentagon shape due to all to all potential with the same coefficients for all the robots and (b) in a cross shape due to one agent being less "repulsive" with respect to the others.

EXPERIMENTAL RESULTS

In this section numerical values used in the control algorithms are defined. Two cases are considered, first the switching of the formation from a pentagon to a cross shape, and secondly the case of a cross formation rotating about its centre. In order to obtain the desired spacing, Equation 8 was solved for Ca_{ij} as function of the other parameters, including the distance amongst the robots, that is considered as the design distance, referred to the case of a 5 robot cross formation. The same values were used for parameters Cr_{ij} and La_{ij}, regardless of the indexing and assumed to be the same for all the interactions amongst the robots, except the ones sensed by one agent. As the testbed labels the robots consecutively (i.e. from 1 to 5), agent number 1 was given a reduced value for Lr_{ij}, in the following referred to as Lr'. Numerical values used, for a cross arm of 700 mm are reported in Table 1

Ca	*Cr*	*La*	*Lr*
99.9996	100	700	698 ***Lr'***=69.8

Table 1. Numerical values of coefficients used in numerical simulations referred to a cross formation with a arm of 700 mm.

A series of tests was performed to validate the switching and the rotational behaviours that the system exhibit when the value of *Lr* parameter sensed by one agent drops to *Lr'* and when the coupling to the centre of mass of the formation is enabled through matrix ***H*** respectively.

Formation Switching

The formation switching was tested using a group of 5 robots randomly deployed in the test area at the beginning of the test. The robots first acquire the pentagon formation, then the *Lr* parameter was manually switched to *Lr'* through the programming interface for the agent that the system labeled as 1. This robot then moved into the centre forcing the others to adjust their distance accordingly, hence surrounding it while achieving a homogeneous spacing amongst them. This is illustrated in Figure 3. The success in the achievement of a static formation was strongly dependent upon the level of accuracy in positioning that was specified. For the case of the 700 mm cross, an accuracy of 20mm was difficult to obtain. This was due to both the noise in measurements and the inherent misalignment between the tracked 6DOF centre and the true kinematic centre of the wheel axes. However the main obstacle to the achievement of a static formation with high accuracy appeared to be the frequency at which the system was updated. As each command maintained execution until a new command was received, the robots may end up with passing from an error in positioning on one side to an error on the other side while trying to correct the first one.

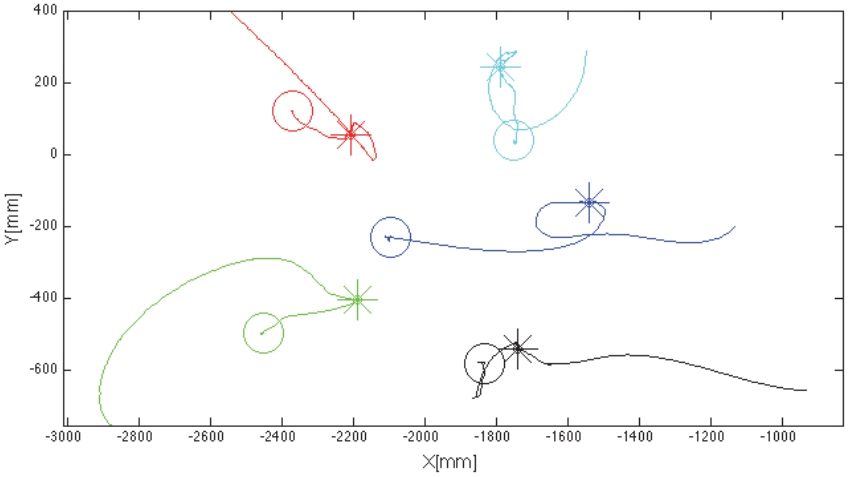

Figure 3. Trajectories followed by the 5 agents while arranging in a pentagon formation first (stars) and then in a cross formation (circles).

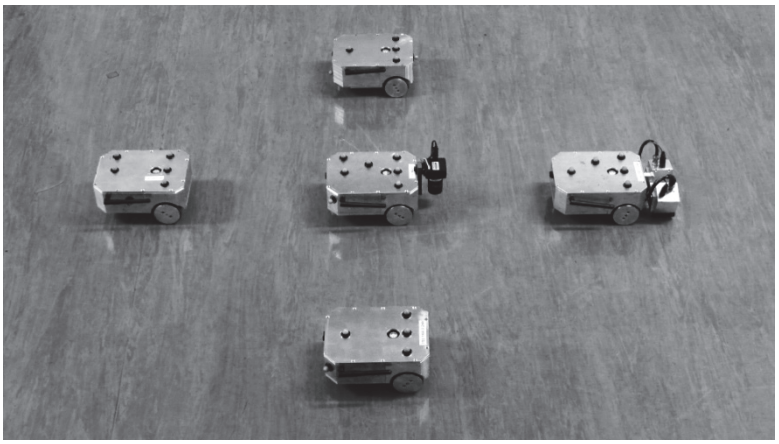

Figure 4. Cross orientation of 5 RSAs.

Rotating Formation

The rotating formation was tested starting from a random arrangement and included both rotation from the beginning of the test, and switching the rotational term when the formation was already stabilised in a cross shape. Figure 5 illustrates the robot paths. The maximum distance between 2 trajectories was always below 40 mm and the formation never acquired a stationary state as to be expected. The failure of one agent was simulated accompanied by a redefinition of $Lr_{ij} = Lr'$ corresponding to the first sorted agent. This shift led the formation to rotate about the new leader (as shown by the shift in centre position of the formation in figure 5).

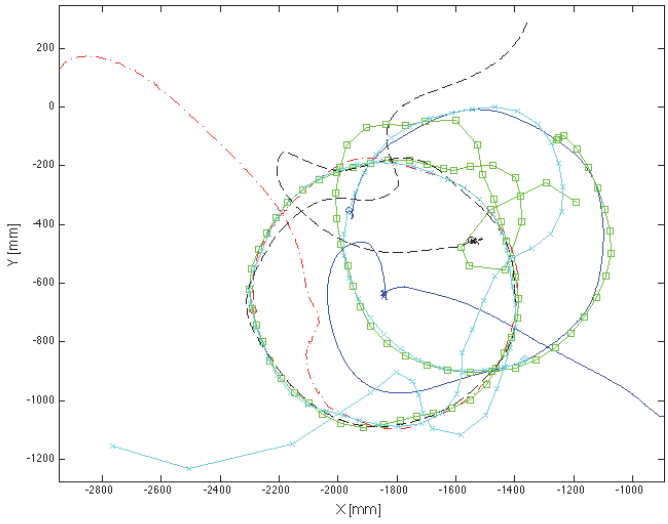

Figure 5: Trajectories followed by the 5 agents while arranging in a cross formation and rotating about its centre. The loss of an agent make the system sort again the agents forming a 3 points star rotating about its centre as well.

CONCLUSIONS

The paper has introduced the use of artificial potential functions (APFs) to generate reconfigurable spatial behavior in a set of five RSA robots developed for Non-Destructive Evaluation (NDE) and health monitoring. Using a photogrammetric tracking system (Vicon T160), it was possible to experimentally evaluate the performance of the APF theory presented. Simple 5-fold symmetries were investigated through a regular pentagon and a cross, and formation switching between the two was implemented as well as demonstrating formation rotation. The relevance of such dynamic swarm behavior in health monitoring applications lies in the applications of *foraging and coverage* and *flocking and formation* behavior in robotically delivered NDE (coverage issues and agent-to-agent based monitoring). Although simple, these standard geometric arrangements form the basis for future investigations into more complex spatial distributions that would support different inspection strategies for the RSA robots.

REFERENCES

1. [Online] UK Research Centre in Nondestructive Evaluation, Available at: http://www.rcnde.ac.uk [Accessed 1st April 2012]
2. Pierce SG, Worden K, Summan R, Dobie G , Hensman JJ, "Towards implementation of reconfigurable robotic strategies for structural health monitoring," 5th European Workshop on Structural Health Monitoring, June 29th 2010, Sorrento, Italy.
3. Friedrich M, "Design of Miniature Mobile Robots for Non-Destructive Evaluation," PhD thesis, University of Strathclyde, 2007.
4. Friedrich M, Pierce SG, Galbraith W, Hayward G, "Data Fusion in Automated Robotic Inspection Systems", Insight, British Institute of NDT, Vol 50 (2), February 2008.
5. Pierce SG, Dobie G, Summan R, Mackenzie L, Hensman JJ, Worden K, Hayward G, "Positioning Challenges in Reconfigurable Semi-autonomous Robotic NDE Inspection," SPIE Smart Structures & Materials & Non destructive evaluation and health monitoring San Diego, CA, 7 - 11 March 2010
6. Summan R, Hensman JJ, Dobie G, Pierce SG, Worden K,"A Probabilistic Approach to Robotic NDE Inspection", Review of Progress in Quantitative Nondestructive Evaluation, QNDE 2009.
7. Thrun S, Burgard W, Fox D. "Probabilistic Robotics-Intelligent Robotics and Autonomous Agents," MIT Press 2005.
8. Harper, C.J., and Winfield, A.F.T., 'A methodology for provably stable behaviour-based intelligent control', Robotics and Autonomous Systems, 54 (1), pp. 52-73, 2006.
9. McQuade, F., Ward, R., Ortix, F., and McInnes, C.R., 'The autonomous configuration of satellite formations using generic potential functions', Third International Workshop on Satellite Constellations and Formation-Flying, Pisa, 2003.
10. McInnes, C.R., 'Velocity field path-planning for single and multiple unmanned aerial vehicles',Aero. J., 107, pp. 419-426, 2003.
11. Reynolds, C.W., 'Flocks, herds, and schools: a distributed behavioral model', Computer Graphics, 21(4) (SIGGRAPH '87 Conference Proceedings) pp. 25-34, 1987.
12. Spears, W. D., Spears J., Hamann, J.C., and Heil, R., 'Distributed, physics-based control of swarms of vehicles', Autonomous Robots, 17(2-3), pp. 137-162, 2004.
13. Parker LE, "Multiple mobile robot systems," in Handbook of Robotics, Bruno Siciliano & Oussama Khatib (Eds.), Springer 2008.
14. Dobie G, "Ultrasonic Sensor Platforms for Non-Destructive Evaluation," PhD thesis, University of Strathclyde, 2010.